Hindawi
Scientific Programming
Volume 2022, Article ID 6180618, 10 pages
https://doi.org/10.1155/2022/6180618

Research Article

Dynamic Planning of Aircraft Sortie Generation Based on Multiobjective Optimization

Xianglei Meng, Nengjian Wang, Jue Liu, and Qinhui Liu

College of Mechanical and Electrical Engineering, Harbin Engineering University, Harbin 150001, China

Correspondence should be addressed to Qinhui Liu; liuqinhui@hrbeu.edu.cn

Received 7 December 2021; Revised 4 January 2022; Accepted 7 January 2022; Published 4 February 2022

Academic Editor: Sheng Bin

The ability of ensuring the safety and reliability of combat aircraft in noncombat processes is a must for aircraft sortie generation. How to guarantee the operation safety and reliability of combat aircraft while ensuring operation efficiency in the air is a matter requiring further exploration and research. For this reason, this paper carries out dynamic planning of aircraft sortie generation based on multiobjective optimization. First, this paper selected a few indicators for measuring the congestion of air field and constructed a state demarcation model; then, it constructed an operating state identification model for the sortie generation and established objective functions for the aircraft runway sequencing model based on the scheduling time span and takeoff and landing delay time loss of the aircraft. At last, this paper elaborated on the methods of landing aircraft parking space scheduling and runway optimization, and the effectiveness of the general model was verified by experimental results, which can be applied to both field-based and cargo-based aircraft sortie generation problems.

1. Introduction

Aircraft sortie generation is an indispensable capability for both air force and navy to fight over long ranges, and it plays an important role in national defense [1–7]. The main functions of aircraft sortie generation should include operating, maintaining, and supporting the takeoff and landing of aircraft concurrently [8–13]. Therefore, it is crucial to ensure the safety and reliability of combat aircraft during sortie generation processes and the movement of landing and flying aircraft on the air field in real time must be checked [14–17]. The existing literature has analyzed the operation process and indices of the aircraft sortie generation and looked for the stochastic evolution law of aircraft operations based on the analysis and mining of the correlations between operation indices [18–20]. Compared with the above research, more in-depth studies are wanted to guarantee the safety and reliability of the aircraft in the complex environment with limited space constraints while ensuring their movement efficiency in the air.

Improving the combat effectiveness of the air field has an important impact on the combat capability of the aircraft sortie generation. In view of the problem of trajectory optimization of aircraft taxiing on the flight ground, Wu et al. [21] introduced the aircraft ground movement model, collision detection strategy, and constraint conditions into the mathematical model, and explained the principle and generality of the chicken swarm optimization algorithm. In order to shorten the support operation time, Jiang et al. [22] considered the topological constraints and resource constraints, established an optimization model of centralized support scheduling for aircraft, proposed a double-population self-adaptive differential evolution algorithm, and verified the feasibility of the model and the validity of the algorithm through comparison and simulation. Based on multibody system dynamics, Min et al. [23] compiled a vessel surface load spectrum, constructed multibody dynamics equations and a simulation model, and proposed a simulation calculation scheme. Shafer et al. [24] studied the aerodynamic ground effect encountered by carrier-based aircraft during carrier landings, and compared with the ground effect present during traditional field-based landings, their research purpose is to quantify the abrupt ground effect for the F/A-18E Super Hornet aircraft. To solve the

uncertainty and dynamic problem about the maintenance and service support, Yuan et al. [25] researched the predictive-reactive scheduling strategy for dynamic support problem, designed a double-population genetic algorithm in predispatching, and integrated the double justification into the evolutionary process of alternating iterations of leftward and rightward populations to improve the global optimality. The automatic landing of aircraft is a complex systematic project. Zhen et al. [26] summarized the development of an automatic landing system and the key techniques of guidance and control for carrier landing, and discussed the basic framework and the operational principle of automatic landing details. Maintenance and service support scheduling for combat aircraft is crucial for the whole cycle of flight and support operations.

In recent years, models established for the dynamic planning of aircraft parking spaces generally took the utilization efficiency of near gate parking spaces and the disturbance of parking spaces as objectives; however, these optimization objectives are mostly about parking spaces, and the overall operation efficiency of the parking area had not been considered comprehensively. Moreover, the current demarcation of the operating state of aircraft is vague, and research on the dynamic and random evolution characteristics of the operating state of aircraft is short. To fill in this research gap, this paper carries out dynamic planning of aircraft sortie generation based on multiobjective optimization. The main content of this paper includes the following aspects: (1) selection of indicators for measuring the congestion of air field and construction of a state demarcation model; (2) construction of an operating state identification model for the sortie generation; (3) construction of objective functions for the aircraft runway sequencing model based on the scheduling time span and takeoff and landing delay time loss of the aircraft; (4) explanation of the methods of parking space scheduling of landing aircraft and runway optimization; (5) verification of the effectiveness of the constructed models using experimental results.

2. Measurement of the Operating State of Sortie Generation

The aircraft sortie generation is a dynamic evolution process. Any change in the operating state of aircraft can directly affect its operating efficiency. This paper divided the operating state of aircraft in the air field into four types: smooth state OS1, stable state OS2, semistable state OS3, and congested state OS4. To give a comprehensive description of the operating state, it is necessary to start from the internal features of the operation sortie generation and establish indicators to measure the congestion of the aircraft operating in the air field. Figure 1 uses a diagram to explain the idea of measuring the operating state of aircraft.

2.1. Selection of Measurement Indicators. The ratio of the difference between the number of landing aircraft w_1 and the number of takeoff aircraft w_2 of the air field within a unit time period to the number of takeoff aircraft can be defined as the detention indicator for measuring the operating state of the air field. This indicator can reflect the current operating state, the dynamic transformation process of the congestion and dispersion of aircraft, and the operating efficiency of the air field. Let w_1 and w_2 be the number of aircraft landing on and taking off from the deck per unit time, respectively. Formula (1) is the calculation formula of detention degree DE:

$$\mathrm{DE} = \frac{w_1 - w_2}{w_2}. \tag{1}$$

According to this formula, the greater the degree of detention, the more prone to aircraft congestion in the air field.

The root cause of aircraft congestion is the imbalance between aircraft landing demand and field capacity. The saturation indicator can simultaneously describe the load level of the air field and the law of congestion. The ratio of the aircraft landing demand W is within a unit time period to the field capacity. D can be defined as the saturation degree of the air field, denoted as ε; formula (2) below gives its calculation formula:

$$\varepsilon = \frac{W}{D}. \tag{2}$$

In order to accurately measure the balance between aircraft landing demand and field capacity and reflect the overall capacity in real time, this paper introduced the indicator of the maximum traffic volume, which is used to describe the maximum number of landing and takeoff aircraft. Assuming that w_{hm} represents the data of the i-th traffic flow in time period h, and $w_{i-\max}$ represents the maximum traffic flow of the carrier deck in time period h, thenthere is

$$w_{h,\max} = \max\{w_{h1}, w_{h2}, \ldots, w_{hi}\}. \tag{3}$$

2.2. Construction of the State Demarcation Model. Then, with the help of qualitative and quantitative analysis, a model was constructed to measure the correlation between the aircraft landing time difference and the air field congestion. In the terminal area of the air field, the aircraft enters the runway at a constant speed and a decelerated speed alternately, and the time it reaches the landing point P is the arrival time of the aircraft. Assuming that μ_{IN} is the aircraft landing rate on the first node of the carrier deck, then the aircraft landing time difference f_{IN} obeys the negative exponential distribution that is suitable for situations with small traffic flow and low density. Assuming that the arrival time of the aircraft is h_i ($i = 1, 2, \ldots, m$), then the time interval between the arrival of the i-th aircraft and the arrival of the $i+1$-th aircraft is $f_i = h_{i+k} - h_i$; the corresponding density function is shown as the formula below:

$$g(f_{\mathrm{IN}}|\mu_{\mathrm{IN}}) = \mu_{\mathrm{IN}} e^{-\mu_{\mathrm{IN}} f_{\mathrm{IN}}}, \quad f_{\mathrm{IN}} \geq f_{\mathrm{IN-min}}. \tag{4}$$

According to above formula, the smaller the aircraft landing time difference, the greater the μ_{IN}; and the greater

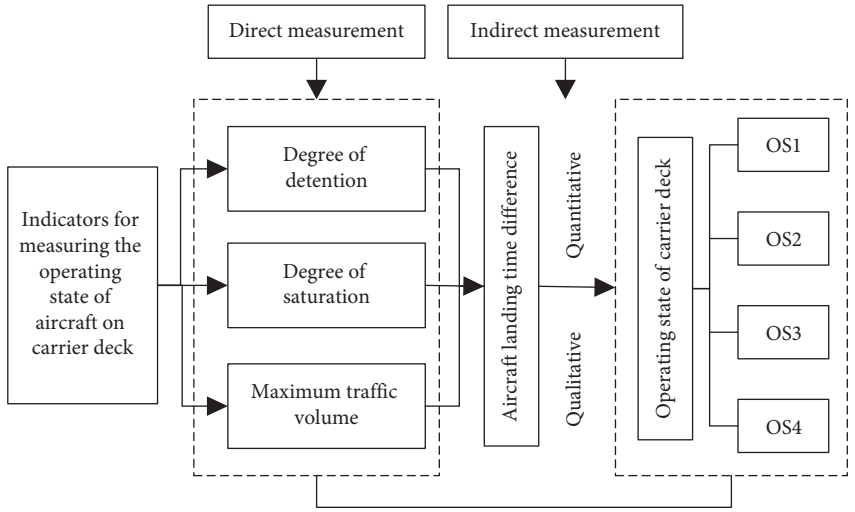

Figure 1: Measurement of operating state of aircraft in air field.

the aircraft landing time difference, the smaller the μ_{IN}. Based on the maximum likelihood estimation method, the estimated value of μ_{IN} could be obtained; formula (5) gives the expression of the likelihood function:

$$\kappa(\mu_{\mathrm{IN}}) \triangleq \prod_{i=1}^{m} g(f_{\mathrm{IN}}|\mu_{\mathrm{IN}}) = \mu_{\mathrm{IN}}^{m} e^{-\mu_{\mathrm{IN}} \sum_{i=1}^{m} f_{\mathrm{IN}}-i}. \tag{5}$$

Order:

$$\frac{\delta\kappa\left(\widehat{\mu}_{\mathrm{IN}}\right)}{\delta\left(\widehat{\mu}_{\mathrm{IN}}\right)} = 0. \tag{6}$$

Formula (7) shows the expression of the maximum likelihood estimate:

$$\widehat{\mu}_{\mathrm{IN}} = \frac{1}{\overline{f}_{\mathrm{IN}}}. \tag{7}$$

Assuming that $f_{\mathrm{IN}-1}$ represents the aircraft landing time difference within time period h, then there is

$$\overline{f}_{\mathrm{IN}} = \frac{1}{m} \sum_{i=1}^{m} f_{\mathrm{IN\text{-}1}}. \tag{8}$$

Since the distribution of aircraft landings obeys the Poisson distribution, then the probability of arriving l aircraft within the time period h can be calculated using the formula below:

$$GV(l) = \frac{(\mu_{\mathrm{IN}} h)^{l} e^{-\mu_{\mathrm{IN}} h}}{l!} = \frac{\left(h/\overline{f}_{\mathrm{IN}}\right) e^{h/\overline{f}_{\mathrm{IN}}}}{l!}. \tag{9}$$

Formula (10) gives the calculation formula for the average number of arrived aircraft within time period h:

$$W_{\mathrm{IN}} = \overline{l} = \sum_{i=1}^{m} l_i GV(l_i) = \sum_{i=1}^{m} l_i GV(l_i) \left(l_i \cdot \frac{\left(h/\overline{f}_{\mathrm{IN}}\right)^{l} e^{h/\overline{f}_{\mathrm{IN}}}}{l!} \right). \tag{10}$$

The retention rate intuitively reflects the difference between landings and takeoffs. If the retention rate DE on the deck is smaller than zero, the deck operates smoothly; if DE = 0, the deck operation is stable; if DE > 0, the deck operation is disorderly unstable. Combining formulas (1) and (10), the DE in the period h can be expressed as

$$DE = \frac{W_{\mathrm{IN}} - W_{\mathrm{LEAVE}}}{W_{\mathrm{LEAVE}}}. \tag{11}$$

The number of landings and takeoffs of the overall runway system, the number of parking spaces, the field capacity, and the aircraft takeoff and landing plan, together determine the saturation degree of the air field. In order to obtain comprehensive and reasonable calculation results of the saturation degree, this paper is combined with the operating characteristics of the air field to calculate the landing and takeoff demands and its capacity. Assuming that D_{IN} represents the aircraft landing capacity and D_{LEAVE} represents the aircraft takeoff capacity, then the relationship between the aircraft landing time difference and the saturation degree can be described by the following formula:

$$\varepsilon = \frac{W_{\mathrm{IN}} + W_{\mathrm{LEAVE}}}{D_{\mathrm{IN}} + D_{\mathrm{LEAVE}}}. \tag{12}$$

For a limited air field space, the greater the maximum traffic volume, the greater the operating pressure. The time segment [0, h] can be equally divided into M subsegments. Assuming that $w_i(h)$ represents the real-time parking space capacity at the beginning of the i-th time segment, $W_{\mathrm{IN}\text{-}i}(s)$ represents the number of aircraft landing within the i-th time segment, and $W_{\mathrm{LEAVE}\text{-}i}(h)$ represents the number of aircraft taking off within the i-th time segment, then by combining formula (3) with formula (10), the relationship between the aircraft landing time difference and the maximum traffic volume could be obtained as shown in formula:

$$w_{i,\max} = \max\left(w_i(h) + W_{\mathrm{IN}\text{-}i}(h) - W_{\mathrm{LEAVE}\text{-}i}(h)\right). \tag{13}$$

By simplifying the above formula, there is

$$w_{i,\max} = \max\left(\sum_{i=1}^{m}\left(W_{\text{IN-}i}(h) - W_{\text{LEAVE-}i}(h)\right)\right). \quad (14)$$

2.3. Construction of the State Identification Model. In order to make a reasonable and effective dynamic plan for aircraft landing on and taking off, this paper used the aircraft landing time difference to define the operating state. First, the operating state was divided quantitatively using a self-organizing neural network, and then, based on the state indicator, the thresholds between the operating states were determined. Assuming that o_{i1}, o_{i2}, and o_{i3} are thresholds corresponding to the functions of retention, saturation, and maximum traffic volume, then formula (15) gives the function describing the operating state identification model:

$$g_i = \begin{cases} OS1, & \overline{M} > o_{i3} \\ OS2, & o_{i2} < \overline{M} \le o_{i3} \\ OS3, & o_{i1} < \overline{M} \le o_{i2} \\ OS4, & \overline{M} \le o_m \end{cases} \quad (15)$$

The weight s_i of each threshold could be determined according to the coefficient of variation, and formula (16) gives the calculation formula of the optimal threshold:

$$o_j = \frac{\sum_{i=1}^{3}\left(o_{ij} * s_i\right)}{\sum_{i=1}^{3} s_i}\ (j = 1, 2, 3). \quad (16)$$

3. The Multiobjective Dynamic Planning of Aircraft Sortie Generation

3.1. Runway Planning. The main purpose of dynamic planning is to make the difference between the actual landing completion time and the estimated landing completion time as small as possible so that the queues at the runways and parking spaces could be reduced, and the overall operating efficiency could be optimized. In this section, with the aircraft scheduling time span and the minimum takeoff and landing delay time loss as the planning principles, the objective function of the runway sequencing model could be established as follows:

Assuming that SM_{iu} represents the start time for aircraft i to occupy runway u, FT_{iu} represents the end time for aircraft i to occupy runway u, d_i represents the unit time delay loss of aircraft i, μ_1 represents the weight coefficient, EH represents the collection of landing aircraft, LH represents the collection of takeoff aircraft, HEM_i represents the actual landing time of aircraft i, HLM_i represents the actual takeoff time of aircraft i, PEM_i represents the estimated landing time of aircraft i, and PLM_i represents the estimated takeoff time of aircraft i, then the objective function can be expressed as

$$\min C_1 = \max FT_{iu} - \min SM_{iu} + \mu_1\left(\sum_{i\in FA} d_i\left|HEM_i - PEM_i\right| + \sum_{i\in LH} d_i\left|HEM_i - PEM_i\right|\right). \quad (17)$$

The scheduling time span in the objective function is represented by $\max FT_{iu} - \min SM_{iu}$. Formula (18) gives the expression of the delay time:

$$\sum_{i\in EH} d_i\left|HEM_i - PEM_i\right| + \sum_{i\in LH} d_i\left|HEM_i - PEM_i\right|. \quad (18)$$

Assuming that g_u^i represents that aircraft i occupies runway u and V represents the collection of the runway time slots and there is $V = \{v_1, v_2, \ldots, v_m\}$, then the constraints of the objective function can be described as follows: formulas (19) and (20) together give the constraint conditions that any aircraft can only occupy one runway for a certain time period for takeoff and landing:

$$\sum_{u\in PD} g_u^i = 1, \quad (19)$$

$$\sum_{y\in v} V_y^i = 1. \quad (20)$$

Assuming that PD represents the collection of runways and v_g represents the minimum safe time interval for a same parking space to park different aircraft consecutively, when two aircraft occupy a same runway one after another, only when the preceding aircraft leaves the runway and the minimum safe time interval is met can the next aircraft enter the runway; these constraints are given by formulas (21) and (22), wherein TY is a sufficiently large positive number:

$$\left|\mathrm{HLM}_{ju} - \mathrm{HLM}_{iu}\right| + \left(1 - f_{ijl}\right)TY \ge v_{g-ij}, \quad \forall i, j \in EH, \forall u \in PD, \quad (21)$$

$$\left|HLM_{ju} - HLM_{iu}\right| + \left(1 - f_{ijl}\right)TY \ge v_{g-ij}, \quad \forall i, j \in LH, \forall u \in PD, \quad (22)$$

where

$$f_{iju} = \begin{cases} 1, & \text{aircraft } i \text{ and } j \text{ occupy runway } u \text{ in sequence.} \\ 0, & \text{otherwise.} \end{cases} \quad (23)$$

Assuming that ψ_{li}^f represents the end time for aircraft i to occupy parking space l, ψ_{xi} represents the taxiing time of aircraft i in the parking area, ψ_i^q represents the waiting time of aircraft i in the parking area, YJ_i represents the estimated taxiing time of aircraft i in the runway area, and the estimated landing time took the sum of ψ_{li}^f, ψ_{xi}, ψ_i^q, and YJ_i, then the formula below gives the constraint that the estimated time for a takeoff aircraft to reach the end of the runway is the estimated takeoff time of the aircraft:

$$PLM_i = \psi_{li}^f + \psi_{xi} + \psi_i^q + YJ_i, \quad \forall i \in LH. \quad (24)$$

To ensure fairness in the dynamic planning of the aircraft runways, the deviation between the actual and estimated takeoff and landing time of the takeoff and landing aircraft should be kept within a reasonable range. Assuming that $LD_{\max}$ represents the maximum lag delay time, then

formulas (25) and (26) give the maximum time offset constraints:

$$0 \le HEM_i - PEM_i \le LD_{max}, \quad \forall i \in EH, \tag{25}$$

$$0 \le HLM_i - PLM_i \le LD_{max}, \quad \forall i \in LH. \tag{26}$$

3.2. Planning of Parking Spaces. The dynamic planning process of aircraft lasts a long time, and the information of aircraft parking requires a frequent and real-time update. Based on the sequencing results of the runway, the aircraft taxiing time can be estimated; then, we can calculate the time for the landing aircraft to arrive at each parking space, and further, the parking spaces could be planned. At the same time, during the parking space planning, the taxiing time of the aircraft, the waiting time in the parking area, and the utilization efficiency of near gate parking spaces could be optimized; that is, to maximize the operation efficiency of the runways under the premise that the utilization efficiency of near gate parking spaces is as high as possible. Figure 2 gives a framework for parking space planning of landing aircraft and runway optimization.

Assuming that *JMP* represents the collection of near gate parking spaces, *YMP* represents the collection of remote parking spaces, K_l^t represents the distance from parking space l to the entrance of the parking apron it belongs, K_l^o represents the distance from parking space l to the exit of the parking apron it belongs, r_i represents the taxiing speed of the aircraft, and μ_1 and μ_2 represent the weight coefficients, then formula (27) gives the objective function:

$$\begin{aligned} \min C_2 = {} & \mu_1 \sum_{l \in YMP} \sum_{i \in EH} a_{il} + \sum_{i \in EH} \left(YJ_i + \frac{K_l^t}{r_i} + \mu_2 \psi_i^q \right) \\ & + \sum_{i \in LH} \left(YJ\psi_i + \frac{K_l^o}{r_i} + \mu_2 \psi_i^q \right). \end{aligned} \tag{27}$$

According to the above formula, the smallest weighted sum of the aircraft taxiing time, the waiting time in the parking area, and the number of aircraft in the remote parking spaces is the template for the planning of parking spaces. Formula (28) gives the constraint that an aircraft can only be allocated to one parking space:

$$\sum_{l \in JMPYYMP} a_{il} = 1, \quad \forall l \in JMPYYMP, \forall i \in EH. \tag{28}$$

Assuming that $T^s_{ai}\psi^v_{li}$ represents the time moment when aircraft i enters parking apron ax and $T^e{}_{ai}\psi^f{}_{li}$ represents the time moment when aircraft i leaves parking apron ax, then formula (29) gives the constraint that the estimated completion time of any landing aircraft is greater than or equal to its actual landing time plus the taxiing time:

$$\psi_{li}^v \ge HEM_i + YJ_i + K_l^t / r_i, \quad \forall i \in EH. \tag{29}$$

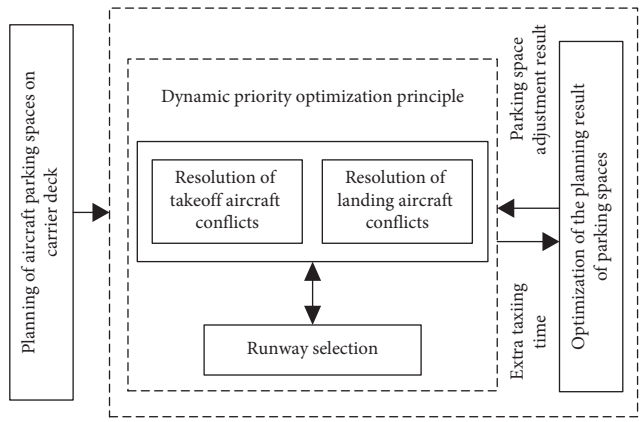

Figure 2: Framework for parking space planning of landing aircraft and runway optimization.

Formula (30) gives the constraint that for one parking space, it can only accommodate one aircraft at a time:

$$\psi_{li}^v \ge \rho_{ijl}\psi_{li}^f + v_g, \quad \forall l \in JMPYYMP, \forall i \in EH, \forall j \in LH. \tag{30}$$

Assuming that h_v represents the minimum transit time, for any takeoff aircraft, before the landing completion time moment, there should be enough time for ground support services, and the corresponding constraint is given by

$$\psi_{li}^v \ge \psi_{li}^f + h_v, \quad \forall l \in \text{JMPYYMP}, \forall i \in LH. \tag{31}$$

The single taxiing path, the densely aircraft parking, and the frequent takeoff and landing planning have resulted in the great possibility of potential risks. Figure 3 gives a diagram of the taxiing conflict of landing aircraft. Assuming that TY_i represents the model of aircraft i, then formula (32) gives the constraint that the model of aircraft i is not bigger than the allowable volume of parking space l:

$$TY_i \cdot a_{il} \le TY_l, \quad \forall l \in JMPYYMP, \forall i \in EH. \tag{32}$$

Formula (33) gives the constraint that a parking area can only allow the movement of one aircraft in a same time period:

$$b_{ijx}\psi_{xi}^f \le \psi_{xj}^v, \quad \forall x \in TJ, \forall i \in EH. \tag{33}$$

The binary function in the formula can be expressed as

$$\begin{aligned} a_{il} &= \begin{cases} 1, & \text{aircraft } i \text{ is assigned to parking space } l, \\ 0, & \text{otherwise}, \end{cases} \\ \rho_{ijl} &= \begin{cases} 1, & \text{aircraft } i \text{ and } j \text{ occupy runway } l \text{ in sequence}, \\ 0, & \text{otherwise}, \end{cases} \\ b_{ijx} &= \begin{cases} 1, & \text{aircraft } i \text{ and } j \text{ occupy parking space } x, \\ 0, & \text{otherwise}. \end{cases} \end{aligned} \tag{34}$$

For ψ_{xi}^v and ψ_{xi}^f, there are

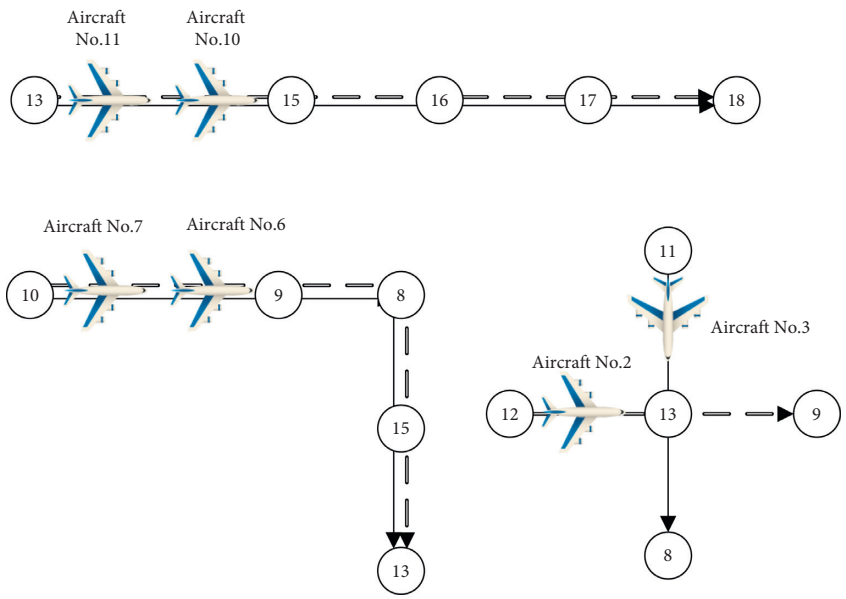

Figure 3: A diagram of taxiing conflict of landing aircraft.

$$\psi_{xi}^{v} = \begin{cases} h_{io}', i \in EH, \\ \psi_{li}^{s}, i \in LH, \end{cases}$$

$$\psi_{xi}^{f} = \begin{cases} \psi_{li}^{v}, i \in EH, \\ \psi_{li}^{f} + \dfrac{K_l^o}{r_i}, i \in LH. \end{cases} \tag{35}$$

3.3. Joint Dynamic Planning. Figure 4 shows the structure of the joint dynamic planning model for runways and parking spaces. Assuming that T represents a sufficiently large positive number and ξ represents the number of violations of the maximum lag constraints as shown in formulas (25) and (26), then formula (36) gives the penalty coefficient of the objective functions for violating the maximum lag constraints:

$$\min C_i' = \max FT_{iu} - \min SM_{ju} + \mu_1 \left(\sum_{i \in EH} d_i \left| HEM_i - PEM_i \right| + \sum_{i \in LH} d_i \left| HLM_i - PLM_i \right| \right) + T * \xi. \tag{36}$$

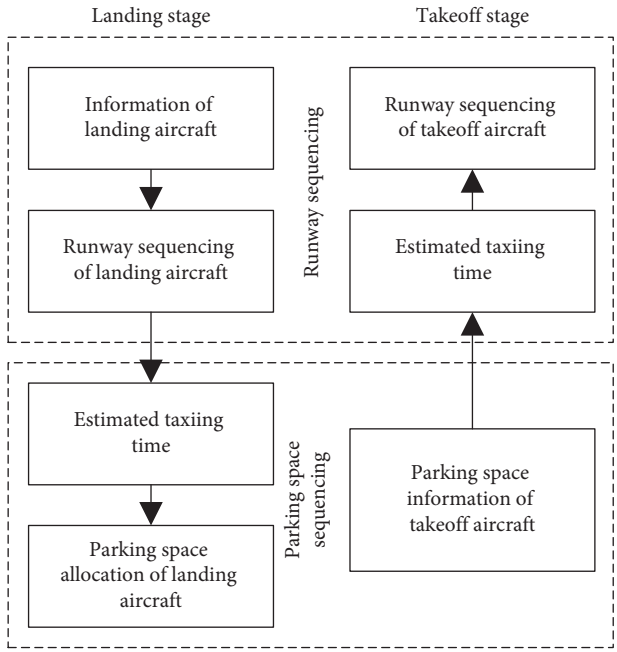

Figure 4: Structure of the joint dynamic planning model for runways and parking spaces.

4. Experimental Results and Analysis

Mimicking the daily landing and takeoff states of aircraft sortie generation, this paper constructs a realistic operation model of aircraft carrier runways and generates statistically meaningful operation data. For example, on a particular day, the number of times of landings and takeoffs of aircraft is 398, and the specific situations of the landing time difference and takeoff time difference of the aircraft on the carrier are given in Figure 5, and Figure 6 shows the frequency distribution of landing time difference of aircraft.

According to Figure 6, we can see that the fluctuation ranges of the landing time difference and takeoff time difference of aircraft were relatively large; most data of the landing time difference and takeoff time difference were within the range of 0–8 minutes; the landing time difference of aircraft was mainly concentrated within the range of 0–8 minutes; the average landing time difference of the aircraft was 6.24 minutes. Based on the above data, the detention degree, saturation degree, and maximum traffic volume of air field were calculated using the methods proposed in this

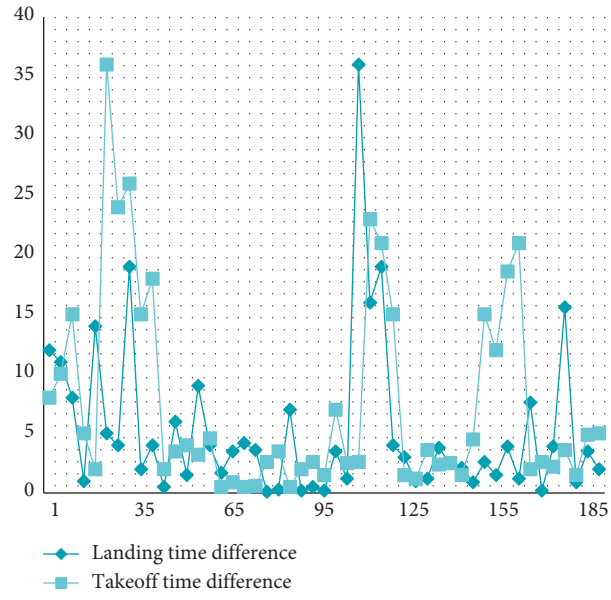

Figure 5: Landing time difference and takeoff time difference of aircraft.

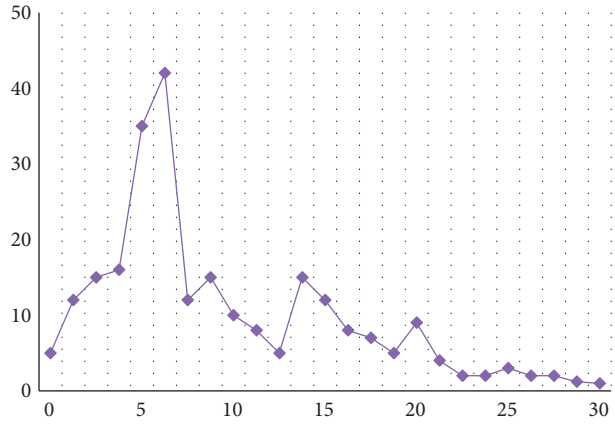

Figure 6: Frequency distribution of landing time difference of aircraft on the carrier.

paper. In order to analyze the changes of these three parameters over time, the data of the takeoffs and landings of aircraft for seven days were processed and analyzed in hours. Table 1 lists the standards for the classification of the operating state.

Figure 7 shows the saturation of the parking spaces in the air field. As can be seen from the figure, there are certain differences in the trend of the saturation value on each day, but their overall trends were the same, and the peak hours were from 14:00 to 18:00. In addition, the saturation of air field did not change much since there is not much difference in the daily noncombat training arrangement during the 7 days; the daily operation was relatively stable, and the effect of dynamic planning was less affected by the external interference. The change trends saturation and the other two parameters (detention degree and maximum traffic volume) were basically the same; when the detention degree was higher, the saturation degree and maximum traffic volume were greater as well. At the same time, when congestion appeared, the change in the detention degree of aircraft was more obvious than that in the saturation degree of parking spaces.

Figure 8 compares the total landing delay time under different dynamic planning strategies (the "first come, first served" method and the genetic algorithm). According to the figure, although for a small number of aircraft, the total delay time had increased; for most aircraft, the total delay time had been reduced. The completion time of the dynamic planning under the two strategies was counted, and the total landing delay time of the aircraft is shown in Table 2.

Any landing aircraft preferentially took the near gate parking space without considering the impact on other landing aircraft. When there are sufficient resources and there are a few conflicts, most aircraft could taxi without conflict. In such a case, the optimal solution appeared in the 150th iteration of the genetic algorithm, and the error of total landing time was maintained at 2110 s. Since the runway taxiing time can hardly be estimated, the optimization degree of the total taxiing time of the aircraft was not high. Because the estimated taxiing time needs to be maximized to ensure that the aircraft will not miss the time slot of the runway, there is a significant negative correlation between the total taxiing time and the total landing time of the aircraft. In the optimal solution, all aircraft can taxi without conflicts during takeoff and landing; among them, 18 aircraft can realize the shortest path to the parking spaces, and the rest of the aircraft can realize a shorter path that effectively avoids conflicts.

Table 3 shows the results of the dynamic planning of aircraft parking spaces. According to the table, after the solution algorithm completes 100 iterations, the estimated waiting time of the parking spaces tends to 0, indicating that at this time, all aircraft have been allocated to vacant parking spaces by the dynamic planning.

The extra taxiing time of some aircraft was relatively long, and the dynamic planning results were further optimized using the method proposed in this paper; after the optimization, the extra taxiing time of each aircraft is shown in Figure 9.

In the optimized parking space planning result, only the No. 35 aircraft and the No. 13 aircraft had exchanged their parking spaces; compared with the original planning result, there is only a small difference. After optimization, the extra taxiing time of the No. 40 aircraft had increased, but the extra taxiing time of the No. 35 aircraft was reduced; for most aircraft, the extra taxiing time can be kept within 40 s, and the total extra taxiing time had decreased from 204 s to 155 s, and all aircraft had maintained good operating and training efficiency. Moreover, the total execution time of the simulation program of the aircraft parking space planning and runway optimization was 367 s, and the total execution time of the simulation program of the joint optimization model was 413 s, which had verified that the calculation speed of the constructed models can meet the actual dynamic planning requirements.

Table 1: Standards for the classification of the operating state.

	Operating state	Detention degree	Saturation degree	Maximum traffic volume
Type	Smooth–stable	−0.30398	0.45201	9.05002
	Stable–semistable	0.15801	0.60173	14.78012
	Semistable–congested	0.38289	0.80112	20.41423

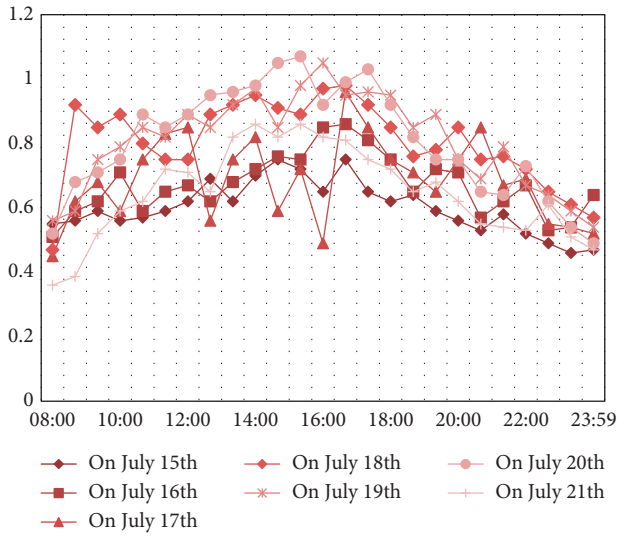

Figure 7: Saturation of parking spaces in the airfield.

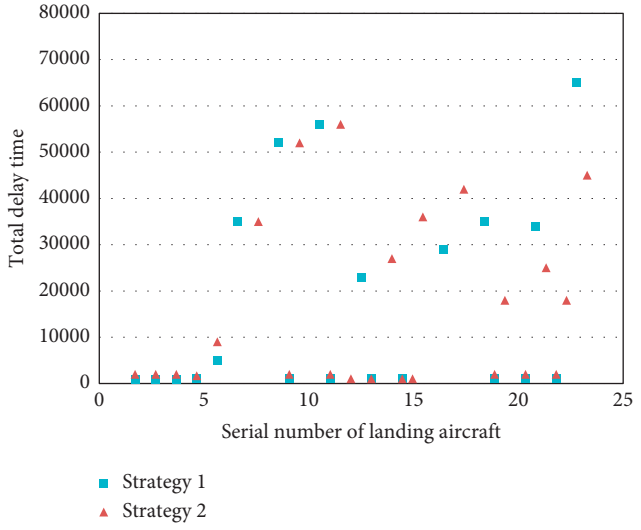

Figure 8: Comparison of total landing delay time under different dynamic planning strategies.

Table 2: Total landing delay time of aircraft.

Aircraft no.	1	2	3	4	5	7	8	9	11	12	13	17
Delay time	285	65	20	66	281	55	63	180	97	94	42	3
Aircraft no.	19	22	24	25	24	25	31	32	31	35	36	37
Delay time	52	25	59	84	27	130	42	39	84	79	106	65

Table 3: Results of dynamic planning of aircraft parking spaces.

Aircraft no.	7	11	13	14	16	17	20	21	26
Planned parking space	p_{12}	p_{18}	p_{13}	p_{16}	p_9	p_1	p_2	p_8	p_{15}
Aircraft no.	29	27	32	33	34	38	41	42	43
Planned parking space	p_{17}	p_5	p_{14}	p_3	p_4	p_6	p_{11}	p_{10}	p_7

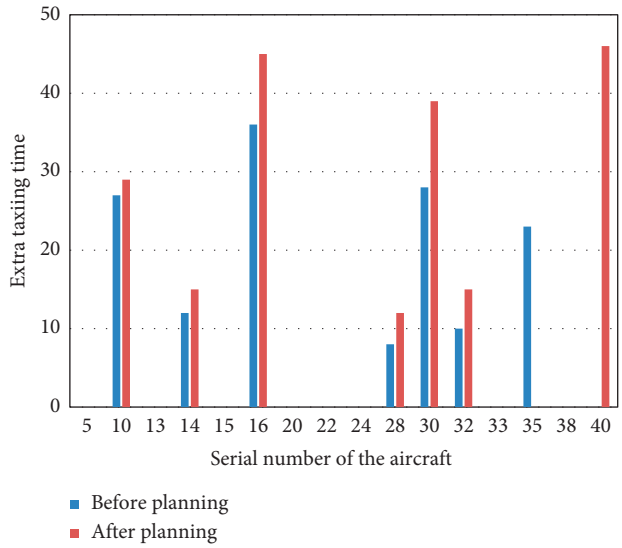

Figure 9: Comparison of extra taxiing time of each aircraft before and after dynamic planning.

5. Conclusion

Based on multiobjective optimization, this paper studied the problem of the dynamic planning of aircraft sortie generation. At first, a few indicators for measuring the congestion situation of aircraft in the air field were selected. Then, a state demarcation model and a sortie generation operating state identification model were established, and objective functions of the aircraft runway sequencing model were constructed based on the scheduling time span and takeoff and landing delay time loss of the aircraft. After that, this paper elaborated on the methods of landing aircraft parking space planning and runway optimization. Through the experiment, the landing time difference and takeoff time difference of the aircraft were counted and analyzed, the saturation of the parking spaces on the carrier deck was plotted into a figure, and the total landing delay time under different dynamic planning strategies was compared and analyzed. At last, the situation of the total landing delay time of the aircraft was given, the extra taxiing time of each aircraft before and after the dynamic planning was compared, and the results had proved that the planning performance and calculation speed of the constructed models can meet the actual dynamic planning requirements. Further, our optimized sortie generation is a general model, and it can be applied to both field-based and cargo-based aircraft sortie generation processes.

Data Availability

The data used to support the findings of this study are available from the corresponding author upon request.

Conflicts of Interest

The authors declare that they have no conflicts of interest.

References

[1] A. K. Bhatia, J. Ju, Z. Ziyang, N. Ahmed, A. Rohra, and M. Waqar, "Robust adaptive preview control design for autonomous carrier landing of F/A-18 aircraft," *Aircraft Engineering & Aerospace Technology*, vol. 93, no. 4, pp. 642–650, 2021.

[2] R. K. Sharma and H. B. Hablani, "High-accuracy GPS-based aircraft navigation for landing using pseudolites and double-difference carrier phase measurements," *IFAC Proceedings Volumes*, vol. 47, no. 1, pp. 200–204, 2014.

[3] R. Thakur and K. V. Kumar, "Investigation of the effect of ski jump on the flow dynamics around generic aircraft carrier," *Defence Science Journal*, vol. 71, no. 2, pp. 296–303, 2021.

[4] J.-L. Hernando and R. Martinez-Val, "Preliminary suitability analysis of carrier approach guidance and recovery of land-based aircraft," *Proceedings of the Institution of Mechanical Engineers - Part G: Journal of Aerospace Engineering*, vol. 230, no. 5, pp. 906–920, 2016.

[5] J. C. Ryan and M. L. Cummings, "A systems analysis of the introduction of unmanned aircraft into aircraft carrier operations," *IEEE Transactions on Human-Machine Systems*, vol. 46, no. 2, pp. 209–220, 2014.

[6] F. Yang, C. Wang, B. Jiang, and S. Huang, "Analysis of reduction in operational capability of aircraft carrier flight deck," *Journal of Harbin Engineering University*, vol. 39, no. 2, pp. 207–214, 2018.

[7] G. Q. Xia, T. T. Luan, M. X. Sun, W. D. Zhong, and Y. W. Liu, "Reduction and catastrophe progression evaluation method

for sortie generation of carrier aircraft," *Mathematical Problems in Engineering*, vol. 40, no. 2, pp. 330–337, 2018.

[8] T. Luan, M. Sun, Z. Hu, Q. Fu, and H. Wang, "A novel TS fuzzy robust control for Part Transportation of aircraft carrier considering transportation time and stochastic demand," *Aerospace Science and Technology*, vol. 2021, p. 2021040420, 2021.

[9] U. Mehta, J. Bowles, S. Pandya et al., "Conceptual stage separation from widebody subsonic carrier aircraft for space access," *Aeronautical Journal*, vol. 118, no. 1209, pp. 1279–1309, 2014.

[10] C. Wang, T. Yang, P. Kulsangcharoen, and S. Bozhko, "An enhanced second carrier harmonic cancellation technique for dual-channel enhanced power generation centre applications in more-electric aircraft," *IEEE Transactions on Industrial Electronics*, vol. 68, no. 7, pp. 5683–5692, 2020.

[11] G. Q. Xia, T. T. Luan, M. X. Sun, and Y. W. Liu, "Research on modeling of parallel closed-loop support process for carrier aircraft based on system dynamics," *International Journal of Control and Automation*, vol. 9, no. 11, pp. 259–270, 2016.

[12] Y. Q. Wang, Y. B. Luo, Q. T. Wang, and Y. Zhang, "Carrier suitability-oriented launch and recovery characteristics of piloted carrier-based aircraft," *Acta Aeronautica et Astronautica Sinica*, vol. 37, no. 1, pp. 269–277, 2016.

[13] A. K. Bhatia, J. Jiang, A. Kumar, S. A. A. Shah, A. Rohra, and Z. ZiYang, "Adaptive preview control with deck motion compensation for autonomous carrier landing of an aircraft," *International Journal of Adaptive Control and Signal Processing*, vol. 35, no. 5, pp. 769–785, 2021.

[14] Q. B. Dou, X. C. Liu, Y. F. G. Xi, Z. C. Yang, and R. K. Mu, "Wing lift simulation method during full scale carrier-based aircraft drop tests," *Journal of Vibration and Shock*, vol. 37, no. 2, pp. 51–56, 2018.

[15] H. Liang, R. J. Mu, D. D. Wang, L. Cai, and L. W. Qiao, "Carrier-aircraft transfer alignment filter based on sparse Gauss-Hermite quadrature algorithm," *Journal of Chinese Inertial Technology*, vol. 22, no. 5, pp. 587–592, 2014.

[16] J. Zhao, G. Sun, S. Zeng, J. Guo, and G. Zhou, "The reliability assessment of human systems interaction for aircraft carrier landing," *Journal of Mechanical Science and Technology*, vol. 30, no. 10, pp. 4465–4469, 2016.

[17] G. X. Xia, R. Dong, J. T. Xu, and X. F. Li, "Linearized carrier-based aircraft model in final approach phase with air turbulence considered," *Acta Aeronautica et Astronautica Sinica*, vol. 37, no. 3, pp. 970–983, 2016.

[18] J. Tian and Y. Dai, "Research on the relationship between mishap risk and time margin for control: a case study for carrier landing of aircraft," *Cognition, Technology & Work*, vol. 16, no. 2, pp. 259–270, 2014.

[19] K. Z. Yue, C. Sun, M. Q. Luo, M. Su, and H. C. Zhao, "Operation model on the carrier warship recovering carrier aircraft," *Systems Engineering and Electronics*, vol. 35, no. 12, pp. 2527–2532, 2013.

[20] Y. Li, Y. Zhu, F. Yang, and Q. Jia, "Inverse reinforcement learning based optimal schedule generation approach for carrier aircraft on flight deck," *Journal of National University of Defense Technology*, vol. 35, no. 4, pp. 171–175, 2013.

[21] Y. Wu, N. Hu, and X. Qu, "A general trajectory optimization method for aircraft taxiing on flight deck of carrier," *Proceedings of the Institution of Mechanical Engineers - Part G: Journal of Aerospace Engineering*, vol. 233, no. 4, pp. 1340–1353, 2019.

[22] T. Jiang, X. Su, and W. Han, "Optimization of support scheduling on deck of carrier aircraft based on improved differential evolution algorithm," in *Proceedings of the 2017 3rd IEEE International Conference on Control Science and Systems Engineering (ICCSSE)*, pp. 136–140, Beijing, China, August 2017.

[23] Q. Min, B. T. Wang, Y. F. Wang, and X. X. Lei, "Compiling load spectrum method for arrested deck-landing of carrier-based aircraft," *Acta Aeronautica et Astronautica Sinica*, vol. 40, no. 4, pp. 26–34, 2019.

[24] D. M. Shafer, B. E. Green, and S. A. Polsky, "Abrupt ground effect of the F/A-18E super Hornet in the aircraft carrier landing environment," *AIAA Scitech 2019 Forum*, vol. 2019, p. 0561, 2019.

[25] P. L. Yuan, W. Han, X. C. Su, and S. H. Gao, "Predictive-reactive dynamic scheduling strategy for carrier aircraft support in uncertain environment," *Systems Engineering and Electronics*, vol. 41, no. 6, pp. 1265–1277, 2019.

[26] Z. Y. Zhen, X. H. Wang, J. Jiang, and Y. D. Yang, "Research progress in guidance and control of automatic carrier landing of carrier-based aircraft," *Acta Aeronautica et Astronautica Sinica*, vol. 38, no. 2, pp. 1–22, 2017.